

Probabilistic forecasting of seasonal drought behaviors in the Huai River basin, China

Mingzhong Xiao^{1,2} · Qiang Zhang^{1,2,3} · Vijay P. Singh⁴ · Xiaohong Chen^{1,2}

Received: 19 June 2015 / Accepted: 6 January 2016 / Published online: 18 January 2016
© Springer-Verlag Wien 2016

Abstract The Huai River basin is one of the major supplier of agricultural products in China, and droughts have critical impacts on agricultural development. Good knowledge of drought behaviors is of great importance in the planning and management of agricultural activities in the Huai River basin. With the copula functions to model the persistence property of drought, the probabilistic seasonal drought forecasting models have been built in the Huai River basin. In this study, droughts were monitored by the Standardized Precipitation Evapotranspiration Index (SPEI) with the time scales of 3, 6, and 9 months, and their composite occurrence probability has been used to forecast the seasonal drought. Results indicated that the uncertainty related to the predicted seasonal drought is larger when more severe droughts occurred in the previous seasons, and the severe drought which occurs in summer and autumn will be more likely to be persistent in the next season while the severe drought in winter and spring will be more likely to be recovered in the subsequent season. Furthermore, given the different drought statuses in the previous season, spatial patterns of the predicted drought events with the largest occurrence probability

have also been investigated, and results indicate that the Huai River basin is vulnerable to the extreme drought in most parts of the basin, e.g., the severe drought in winter will be more likely to be persistent in spring in the central part of the southern Huai River basin. Such persistent drought events pose serious challenges for planning and management of agricultural irrigation, then results of the study will be valuable for the planning of crop cultivation or mitigation of the losses caused by drought in the Huai River basin, China.

1 Introduction

As a prolonged water deficit event, drought has a devastating effect on agriculture, water supply, ecosystem, public health, energy, and the economy, being challenging topics in water resource management. It is estimated that the damages incurred from the drought are far more than other meteorological disasters such as floods and hurricanes, and the US economic losses caused by droughts are as high as 6 to 8 billion dollars each year (Wilhite, 2000). In recent decades, with the population growth and expansion of agricultural, energy, and industrial sectors, it has been found that the demand for water resources has increased many fold and water scarcity has been occurring almost every year in many parts of the world (e.g., Mishra and Singh, 2010). Therefore, there is an urgent need to develop an algorithm for characterizing and predicting droughts; however, this cannot be achieved easily either through physical or statistical analyses (Kao and Govindaraju, 2010).

Unlike other extreme hydrological events such as floods, the evolution of drought is slow, and then an effective mitigation of the most adverse drought impacts is possible based on a timely monitoring of an incoming drought. There are several studies that have focused on drought forecasting, corresponding to the drought indicators computed using dynamic or

✉ Qiang Zhang
zhangq68@mail.sysu.edu.cn

¹ Department of Water Resources and Environment, Sun Yat-sen University, Guangzhou 510275, China

² Key Laboratory of Water Cycle and Water Security in Southern China of Guangdong High Education Institute, Sun Yat-sen University, Guangzhou 510275, China

³ School of Environment and Civil Engineering, Suzhou University, Suzhou, Anhui 234000, China

⁴ Department of Biological & Agricultural Engineering and Zachry Department of Civil Engineering, Texas A & M University, College Station, TX 77843-2117, USA

statistical model, and the drought forecasting is generally categorized as dynamic drought forecasting (e.g., Yuan et al. 2013; Niu et al. 2015) and statistical drought forecasting (e.g., AghaKouchak, 2014; Salvadori and De Michele, 2015); this study focuses on the statistical drought forecasting. Based on the persistence property of accumulated soil moisture, AghaKouchak (2014) found that the 2012 US summer drought was predictable several months in advance with the ensemble streamflow prediction (ESP) method. Recently, the copula functions have been widely used to model the dependence structure between random variables (Nelsen, 2006; Zhang et al. 2012). With the copula function to model the persistence property of the Standardized Streamflow Index (SSI), a probabilistic seasonal drought forecasting method has been proposed by Madadgar and Moradkhani (2013) that a future drought status can be estimated given the earlier drought conditions. It has been found that the results of the new method were generally in agreement with the ESP method; however, the forecast uncertainty of the new method is more reliable than that of the ESP method (e.g., Madadgar and Moradkhani, 2013). Therefore, this method has also been used in this current study.

When a drought event occurs, moisture deficits are observed in many hydrologic variables, such as precipitation, streamflow, and soil moisture. Focusing on the deficits in precipitation, the meteorological droughts have been analyzed in this study. Due to the stochastic nature of water demands in different regions, many drought indices have been developed and applied to quantify and monitor the development of drought. As it is simple to calculate and be able to describe both short-term and long-term drought impacts through various time scales of precipitation anomalies, the Standardized Precipitation Index (SPI) has been widely used (Shiau, 2006; Cancelliere et al. 2007; Kao and Govindaraju, 2010; Zhang et al. 2012; Zhang et al. 2013a; Sanusi et al. 2015). However, the SPI cannot capture the main impact of increased temperatures on water demand, as the evapotranspiration may increase with global warming, then as an extension of the widely used SPI, Vicente-Serrano et al. (2010) proposed the Standardized Precipitation Evapotranspiration Index (SPEI) which is designed to take into account both precipitation and potential evapotranspiration (PET) in determining drought. The SPEI has also been widely used in the analysis and evaluation of drought (Vicente-Serrano et al. 2013; Yu et al. 2014; Zhang et al. 2015). In this case, the SPEI was used in monitoring of droughts in this study.

Furthermore, owing to the various time scales of SPEI, there may be some confusions due to inconsistent results of droughts at different time scales, and this is a major dilemma so far that the drought status being assessed based on one drought index often does not correspond well with that based on different drought index because of complex mechanisms behind occurrence of drought regimes (e.g., Kao and

Govindaraju, 2010). In addition, droughts usually result from cumulative effects of water shortages over different periods of time; it is necessary to clarify information from various sources to successfully assess a drought. Therefore, SPEIs at various time scales were analyzed to formulate a complete picture of drought regimes in the study.

Located in eastern China between the Yangtze and the Yellow River basins, the Huai River basin is the main cropping area in China, accounting for 12 % of the national total arable land. However, due to frequent extreme droughts, the Huai River basin is very vulnerable to drought hazards; it has been found that the recurrent frequency of drought in the Huai River basin is nearly once every 4 years from 1960 to 2009 and the occurrence frequency has increased significantly since 2000 (Yan et al. 2013). In addition, the Huai River basin is densely populated with a population of 16.2 % of the total national population (FAO, 2015); the population density is approximately four times higher than the national average. Due to the critical role of the Huai River basin in the socioeconomic development of China, good understanding of drought behaviors, particularly with the help of improved drought forecasting model, will be of great importance in developing appropriate human mitigation to drought hazards in the Huai River basin. This is the major motivation of this study.

Therefore, the objectives of this study are as follows: (1) to develop a probabilistic forecasting model of seasonal drought based on copula functions and (2) to integrate information of SPEIs with different time scales in both space and time, picturing drought variations across the Huai River basin. This paper is organized as follows: introduction of study region and data is presented in Section 2, and methods of analysis are depicted in Section 3. Results and discussion thereof are described in Section 4, which is followed by Section 5 as the conclusion of this study.

2 Study region and data

The Huai River basin (111° 55' E–121° 25' E; 30° 55' N–36° 24' N) is located in eastern China between the Yangtze River basin and the Yellow River basin (Fig. 1), with the drainage area of 270,000 km². Located in the climate transition zone of China, the annual mean temperature of the Huai River basin ranges from 11 to 16 °C and the long-term annual average precipitation is about 920 mm. Generally, the precipitation decreases from south to north, from the mountainous area to the plains, and from coastal to inland (e.g., Gao et al. 2015). Besides, spatial distribution of precipitation is extremely uneven within a year; about 50–80 % of the annual total precipitation occurs during June and September. The Huai River basin is one of the most important grain-producing regions in China, and there are 12.72 million ha of arable land in 2005, approximately 12 % of China's total arable land. The main crops in the Huai

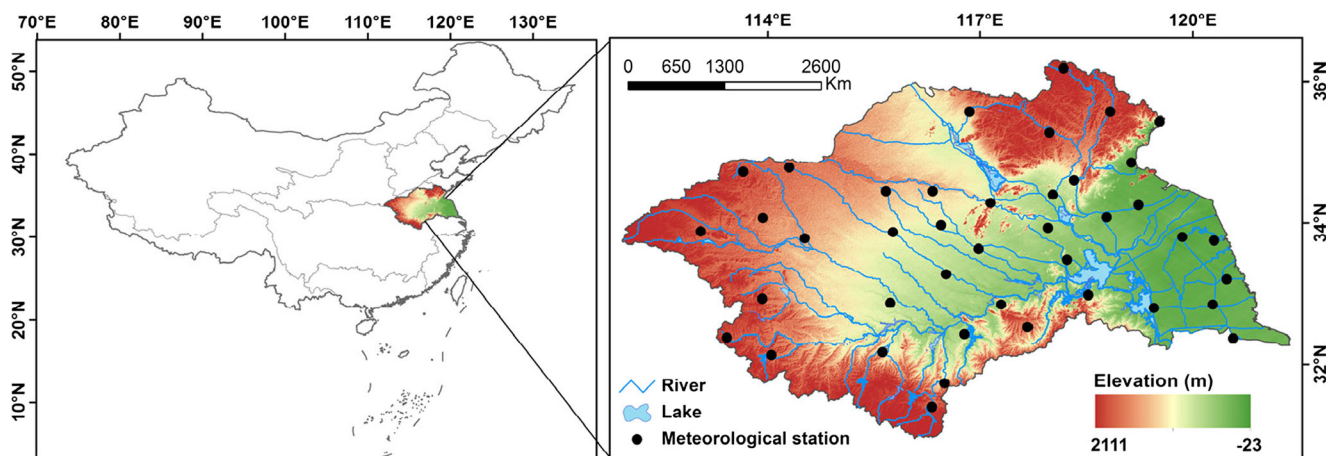


Fig. 1 Locations of the study region, the Huai River basin, and the meteorological stations

River basin are wheat, rice, corn, potato, soybean, cotton, and canola. In addition, the population in the basin is around 170 million, and its population density is approximately four times higher than the national average (Duan et al. 2014). In this sense, thorough investigation of droughts in the Huai River basin is theoretically and practically relevant in social stability and also food security in China.

In this study, daily precipitation and temperature data (maximum and minimum temperature) covering the period of 1960 to 2013 at 41 meteorological stations were collected from the National Meteorological Information Center of the China Meteorological Administration. Locations of meteorological stations can be found in Fig. 1. For daily precipitation dataset, there are four meteorological stations containing missing days with the largest missing rate of 0.47 %. However, for daily temperatures, there are 19 and 24 meteorological stations containing missing days, respectively, for the maximum and minimum temperature, with the largest missing rate of 0.48 %, and most of them had less than 0.01 % of total missing values. The missing data of specific days were filled in by the long-term average value of the same days of other years. In this paper, the probabilistic forecasting models of seasonal drought are calibrated and validated over the periods of 1960–2010 and 2011–2013, respectively.

3 Methodology

3.1 Standardized Precipitation Evapotranspiration Index

The SPEI was proposed by Vicente-Serrano et al. (2010) to represent the true drought conditions of the study region under the influences of warming climate. The SPEI is designed to take into account both precipitation and potential evapotranspiration (PET) in picturing drought, and PET is the amount of evaporation and transpiration that would occur if a sufficient water is available. In the calculation of SPEI, a modified form

of the Hargreaves equation (Hargreaves, 1994; Droogers and Allen, 2002) was used to compute the monthly PET. Then the difference between monthly precipitation (P) and monthly PET for the month i is calculated as $D_i = P_i - PET_i$, which provides a simple measure of the water deficit for the months under consideration. Similar to SPI, the SPEI is also a multi-scalar standard normal drought index, and the calculated D_i values are aggregated at different time scales as follows:

$$D_n^k = \sum_{i=0}^{k-1} D_{n-i} \tag{1}$$

where k is the time scale and n is the time. As suggested by Vicente-Serrano et al. (2010), the three-parameter log-logistic distribution has been selected to model the D^k series. With the cumulative distribution function $F(x)$ of the log-logistic distribution, SPEI was obtained as the standardized value of $F(x)$, and details of the calculation can be referred to Vicente-Serrano et al. (2010). In this study, the SPEI is calculated based on the R package of “SPEI” (Beguería and Vicente-Serrano, 2013). Same as the drought classification for SPI (Madadgar and Moradkhani, 2013; Madadgar and Moradkhani, 2014), the drought classification determined by the U.S. Drought Monitor (<http://droughtmonitor.unl.edu/AboutUs/ClassificationScheme.aspx>) has also been used for SPEI (Table 1).

Table 1 Drought classification for the standardized indices (SI), and there are minor modifications compared to the drought classification defined by the U.S. Drought Monitor

Drought category	Drought severity	SI value
D0	Abnormally dry	(−0.7, −0.5]
D1	Moderate	(−1.2, −0.7]
D2	Severe	(−1.5, −1.2]
D3	Extreme	(−2.0, −1.5]
D4	Exceptional	(−∞, −2.0]

3.2 Copula functions

Copulas are multivariate distribution functions on the n -dimensional unit cube with uniform marginal on the interval $[0, 1]$, that is, $C: [0, 1]^n \rightarrow [0, 1]$. Based on Sklar's theorem (Sklar, 1959), a multivariate distribution $F(x_1, x_2, \dots, x_n)$ can be expressed by a copula as follows:

$$\begin{aligned} F(x_1, x_2, \dots, x_n) &= C[F_{X_1}(x_1), F_{X_2}(x_2), \dots, F_{X_n}(x_n)] \\ &= C(u_1, u_2, \dots, u_n) \end{aligned} \quad (2)$$

where $F_{X_i}(x_i)$, denoted by u_i in the copula definition, represents the marginal distribution of the i th variable and C is the copula cumulative distribution function. Owing to the fact that the copula can model the dependence structure between random variables irrespective of the types of marginal involved, the copula functions have been widely used in various areas (Nelsen, 2006; Zhang et al. 2012; Zhang et al. 2013b; Madadgar and Moradkhani, 2013; Madadgar and Moradkhani, 2014). In this study, six bivariate copula functions from the Archimedean (Gumbel, Clayton and Frank), Elliptical (Gaussian and t), and Plackett copulas have been used to represent the correlation of the drought in two adjacent seasons. Details of these six bivariate copula functions can be referred to Nelsen (2006), Zhang et al. (2013a, b), and Chen et al. (2015).

3.3 Copula fitting

To appropriately join the marginal distributions of dependent variables, a best copula has to be selected from these six aforementioned copula functions. In this study, goodness-of-fit (GOF) tests based on the Cramér-von Mises statistic (S_n) have been used. As a measure of distance between the empirical and parametric copulas (C_{EMP} and C_θ), the S_n is defined as that (Genest et al. 2009; Madadgar and Moradkhani, 2014; Hofert et al. 2015):

$$S_n = \int_u \Delta C(u)^2 dC(u) \quad (3)$$

$$\Delta C = \sqrt{n}(C_{\text{EMP}} - C_\theta)$$

where n is the sample size. The p value of the GOF test is calculated by bootstrap sampling via the Monte Carlo approach (Genest et al. 2009), and 1000 replications have been simulated in this study. For a group of copulas, it is possible that there are several copulas significant at the 95 % confidence intervals, and then the best alternative is the one with the smallest S_n and the greatest p value as suggested by Madadgar and Moradkhani (2014).

Before finding the best choice of copula function, several marginal distributions are tested to fit the seasonal average SPEI generated at each station, and the generalized normal (GN), generalized Pareto (GP), Pearson Type III (P-III), and

generalized extreme value (GEV) distributions have been used in this study with the parameters estimated by the L-moments method. Also as suggested by Madadgar and Moradkhani (2014), the best marginal distribution is selected by the Kolmogorov-Smirnov (K-S) and the Akaike information criterion (AIC) tests. When it passes the K-S test, the distribution with the smallest AIC is selected as the best fit.

3.4 Conditional probability density function

Let X and Y be random variables with marginal distribution as $u = F_X(x)$ and $v = F_Y(y)$, and their dependence structure has been represented by the copula function (C_θ), then the conditional distribution function of X given $Y \leq y$ can be expressed as:

$$C_\theta(u|v) = \frac{C_\theta(u, v)}{v} \quad (4)$$

Similarly, an equivalent formula for the conditional distribution function for X given $y_1 \leq Y \leq y_2$ can be obtained as that (Chen et al. 2015):

$$C_\theta(u|v') = \frac{C_\theta(u, v_2) - C_\theta(u, v_1)}{v_2 - v_1} \quad (5)$$

As the correlation of the drought in two adjacent seasons has been represented by the copula function, the conditional distribution of each seasonal drought given the drought status in the previous season can be calculated in the study. Furthermore, as $u = F_X(x)$, then based on the chain rule of differential, the conditional probability density function can be written as that:

$$f(x|v') = \frac{\partial C_\theta(u|v')}{\partial u} f(x) \quad (6)$$

If there is no analytic formula, the conditional probability density function can also be easily calculated by the numerical methods. What is more, if $y_1 = y_2$, the conditional probability density function of Eq. (6) can be simply written as that:

$$f(x|y) = c(u, v)f(x) \quad (7)$$

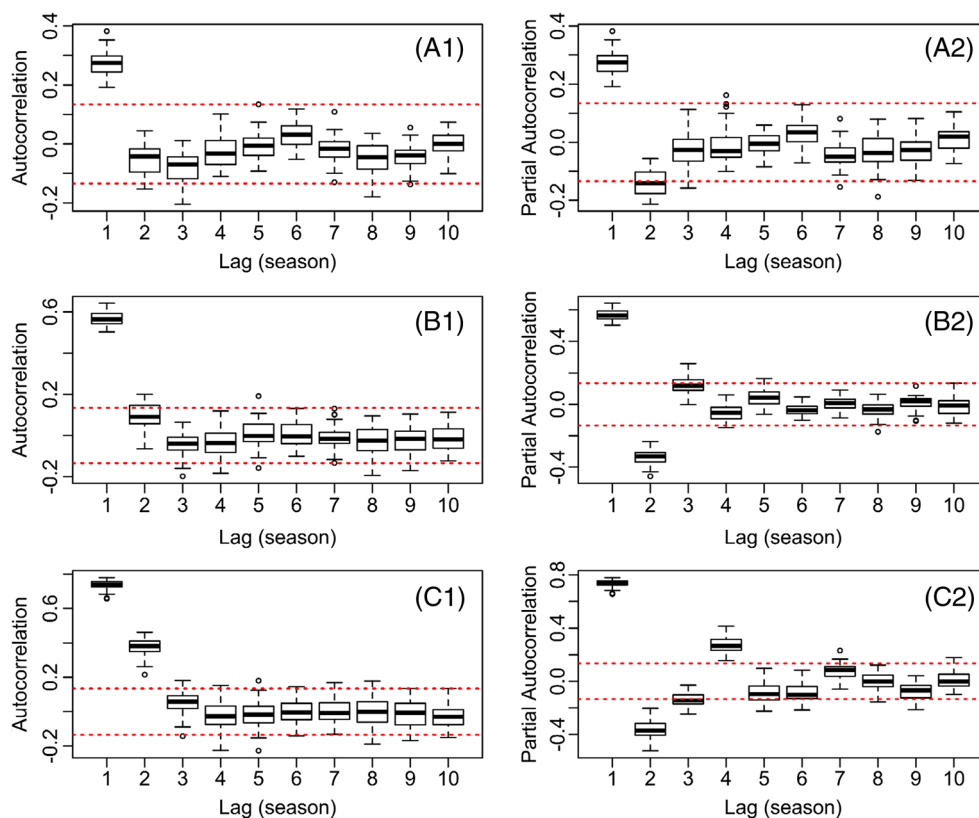
where $c(u, v)$ is the copula density, and this is the same as the equation (9) derived by Madadgar and Moradkhani (2013).

4 Results and discussions

4.1 Selection of the marginal distributions and copula functions

Trying to form an overall judgment of a drought, the SPEI with the time scales of 3, 6, and 9 months (represented as SPEI-3, SPEI-6 and SPEI-9), respectively, have been analyzed in this study. As the seasonal average of monthly SPEI, the

Fig. 2 The boxplot for the autocorrelation and partial autocorrelation of seasonal average SPEI with different time scales. **a** SPEI-3, **b** SPEI-6, and **c** SPEI-9. The thresholds at the 95 % confidence interval are shown as red dotted lines



seasonal SPEIs have been calculated for all of the stations, and the autocorrelation of seasonal SPEI with different time scales have been shown in Fig. 2. It can be expected that the seasonal drought be influenced by the drought status in the previous season and even the previous two seasons for the drought indicated by the SPEI-9. An inspection of Fig. 2 shows that for the SPEI-3 and SPEI-6, only the lag-1 autocorrelation is significant at the 95 % confidence level at most of the stations; this further indicates that the seasonal droughts defined by SPEI-3 and SPEI-6 are influenced by the drought status in the previous season in the Huai River basin. Besides, for the SPEI-9, the autocorrelation of seasonal SPEI-9 (Fig. 2c(1)) generally decreases with the increasing lags while the autocorrelation in the first two lags are significant at the 95 % confidence level. However, the lag-2 autocorrelation may be

influenced by lag-1 autocorrelation. To remove the influence of lag-1 autocorrelation on lag-2 autocorrelation, the partial autocorrelation has been calculated for the seasonal SPEI-9 (Fig. 2c(2)). It can be observed from Fig. 2c(2) that the lag-1 partial autocorrelation is very strong, and the partial autocorrelations gradually taper to 0 thereafter, oscillating between the negative and positive values. So in the paper, only the dependences between two consecutive seasonal droughts have been analyzed, and the dependence structure can be modeled by the copula functions. Based on the goodness-of-fit test introduced in Section 3.3, the selected copula functions have been shown in Table 2. Table 2 indicates that for the SPEI-3, the Gumbel and Clayton copulas perform well in modeling the dependence structures between two consecutive seasonal droughts while the seasonal SPEI-6 and SPEI-9 are

Table 2 Number of stations with the same copula function selected for the dependence between two adjacent seasonal average droughts defined by the SPEI with different time scales

Copula	Winter–Spring			Spring–Summer			Summer–Autumn			Autumn–Winter		
	3M	6M	9M	3M	6M	9M	3M	6M	9M	3M	6M	9M
Gumbel	29	14	10	18	19	5	3	3	9	19	13	4
Clayton	-	4	6	4	3	12	15	3	2	11	4	2
Frank	6	11	2	1	2	4	3	5	5	1	2	2
Gaussian	4	7	16	8	7	11	8	15	19	8	12	11
<i>t</i>	2	1	6	10	8	8	10	14	6	1	10	18
Plackett	-	1	1	-	2	1	1	1	-	1	-	4

Table 3 Number of stations with the same distribution function selected for each seasonal average drought defined by the SPEI with different time scales

Distribution	Spring			Summer			Autumn			Winter		
	3M	6M	9M	3M	6M	9M	3M	6M	9M	3M	6M	9M
GN	11	1	5	4	6	7	10	5	1	11	9	4
GP	-	-	1	2	1	-	-	-	1	-	-	1
P-III	1	3	4	2	3	-	2	17	26	3	3	21
GEV	29	37	31	33	31	34	29	19	13	27	29	15

well represented by the Gaussian and t copulas. Besides, the marginal distributions for the seasonal SPEI-3, SPEI-6, and SPEI-9 have also been selected (Table 3), results indicate that for most of the stations, the seasonal drought can be well pictured by GEV distribution, and the P-III distribution also performs well in describing probability behaviors of SPEI-9.

4.2 The probabilistic forecasting of seasonal drought

For seasonal SPEI-3, SPEI-6, and SPEI-9, given different drought statuses in the previous season, their conditional probability density functions have been calculated, and the regional average probability density distributions of seasonal drought given the severe drought status (D2, referred to the definition in Table 1) in the previous season have been illustrated in Fig. 3. Due to the fact that droughts usually occur as results of cumulative effects of water shortages over different periods, it is necessary to mine information from various sources to successfully assess droughts. Without considering the dependent relationships between SPEI-based droughts at different time scales, the average of SPEI-3, SPEI-6, and SPEI-9 has been calculated as a composite index to formulate an overall judgment of a drought in the study, and the composite probability density distribution was analyzed (Fig. 3). It should be noted here that there are some stations without the

appropriate copula functions to model the dependence between the two adjacent seasonal SPEIs; to avoid bias, they have been neglected in the calculation in the study. It can be seen from Fig. 3 that the conditional probability density functions are narrower with increase of time scale of SPEI, and these can be attributed to the stronger dependence relations between two consecutive seasonal SPEIs when its time scale is larger. As the average of SPEI-3, SPEI-6, and SPEI-9, the modes of the composite probability density distribution can be expected to be strongly affected by the probability density distribution of SPEI-9.

Besides, to validate the probabilistic seasonal drought forecasting models with the composite probability density distributions, the seasonal data from 2011 to 2013 that started with the winter from December 2010 to February 2011 have been used. In this study, the value with the largest probability is selected as the predicted drought with the largest occurrence probability, and the predicted drought in the central 95 % intervals of the probability distribution have also been calculated (Fig. 4). It can be seen from Fig. 4 that the predicted droughts with the largest occurrence probability are in good line with the observed droughts in each season, and almost all of the observed droughts are inside the central 95 % intervals of the predicted drought. Apart from visual examination of the forecast, the Nash-Sutcliffe coefficients have been calculated

Fig. 3 The regional average probability density distribution of drought given the severe drought status (D2) in the previous season. **a** Spring, **b** summer, **c** autumn, and **d** winter. The drought is defined by the SPEI with different time scales, and the composite probability density distribution is also shown as average

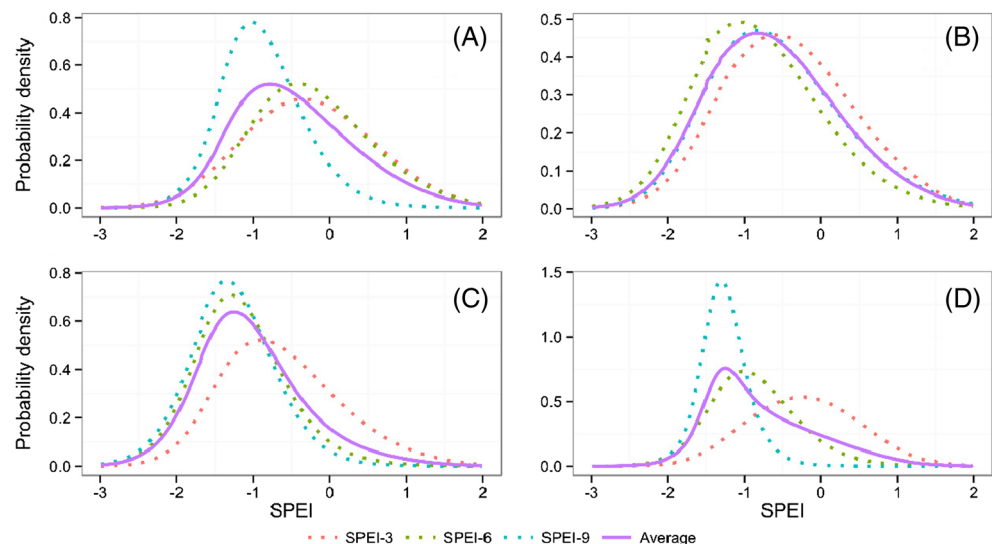
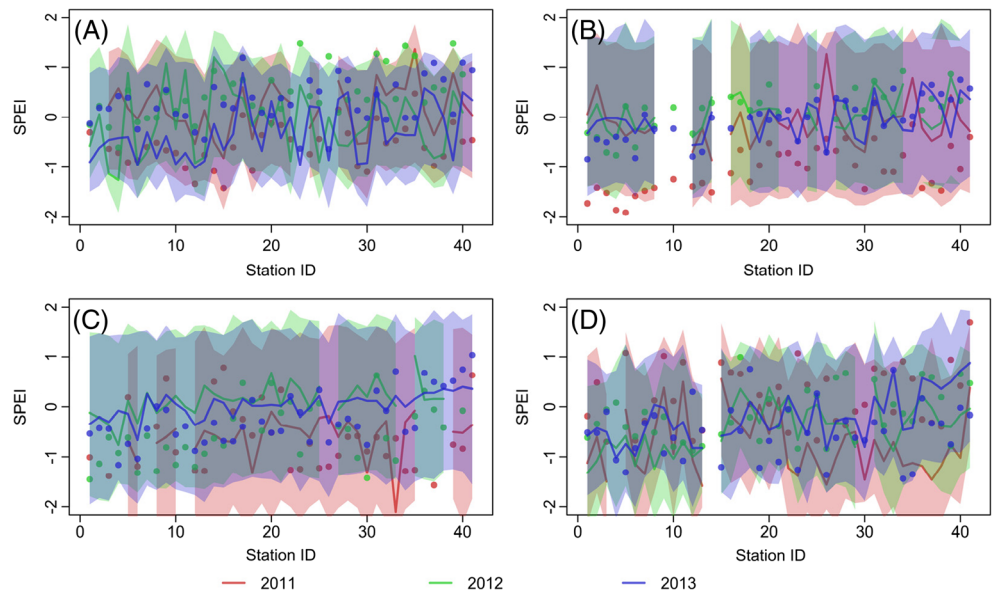


Fig. 4 Validation of probabilistic seasonal drought forecasting model using the data during 2011–2013 at all stations in the Huai River basin: **a** winter, **b** spring, **c** summer, and **d** autumn. The observed drought data are represented by the *points*, the predicted droughts with the highest occurrence probability are denoted by the *lines*, and the predicted drought in the central 95 % intervals of the probability distribution are also shown as *shading*



in the study to further quantitatively assess the accuracy performance for all of the stations during 2011–2013. Unlike the deterministic forecast, the probabilistic forecast provides the information about confidence in the forecast; to calculate the Nash-Sutcliffe coefficients, the predicted droughts are indicated by the value with the largest occurrence probability. Corresponding to the observed mean and naïve prediction, it has been found that the Nash-Sutcliffe coefficients are 0.35 and 0.28, respectively. An efficiency larger than 0 indicates a better predictor than the reference model, and the closer the model efficiency is to 1, the more accurate the model is. So these results indicate that the probabilistic seasonal drought forecasting models for each season work well in the Huai River basin, and the predicted droughts can be used as a reference for the regional water resource management and human mitigation to droughts. It should be noted here that naïve forecasts

are simply the lag-1 backward shifted observations. In Austria, Van Loon and Laaha (2015) found that hydrological drought severity is strongly influenced by climate and catchment characteristics, and the impacts of climate indices such as El Niño–Southern Oscillation (ENSO) and North Atlantic Oscillation (NAO) on drought have also been found in many regions (Bonaccorso et al. 2015; Ma et al. 2015; Wang and Kumar, 2015). So the limitation of the drought forecasting models in the study may be owing to these factors, and these need to be further analyzed.

Based on drought classification as shown in Table 1, five drought statuses have been defined as D0, D1, D2, D3, and D4, representing the drought severity levels from abnormally dry to exceptional, respectively. For each season, given the drought status in the previous season, the composite conditional probability density distributions can be calculated for all

Fig. 5 The composite probability density distribution of seasonal SPEI given the drought status in the previous season. **a** Spring, **b** summer, **c** autumn, and **d** winter. Details of drought status can be found in Table 1

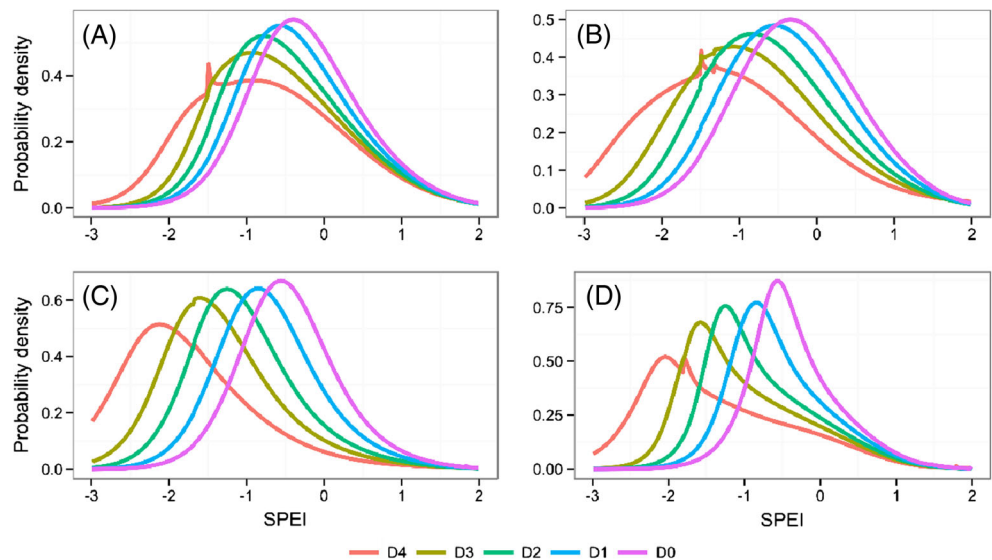
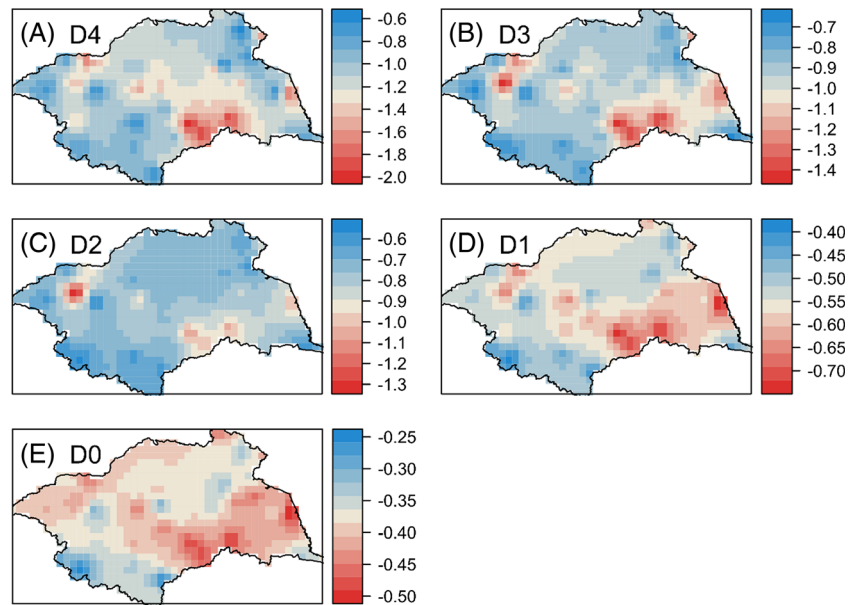


Fig. 6 Spatial distribution of the predicted droughts with the largest occurrence probability in the Huai River basin in spring given the drought status in the previous season (winter in the previous year; **a** D4, **b** D3, **c** D2, **d** D1, **e** D0). Details of drought status can be referred to Table 1, and the *color bar* represents the value of SPEI



the stations. To overall illustrate the correlation of seasonal drought in the Huai River basin, the regional average composite probability density distributions have been calculated for each season (Fig. 5). It can be seen from Fig. 5 that distributions of the conditional probability density distribution are wider when the drought status in the previous season are more severe, which implies that the variability of the predicted seasonal drought is larger when a more severe seasonal drought occurs in the previous season, indicating higher difficulty in drought forecasting. Besides, it can also be seen from Fig. 5 that when the same drought status in the previous season occurs, the drought tends to be more severe in autumn (September, October, and November) and winter (December, January,

and February) while less severe in spring (March, April, and May) and summer (Jun, July, and August), indicating that the severe drought in summer and autumn will be more likely to be persistent in the next season, while the severe drought in winter and spring will be more likely to be recovered in the next season. These changing properties of droughts mean much for management and planning of agricultural irrigation in the Huai River basin, China.

In addition, spatial distributions of droughts with the largest occurrence probability have also been analyzed given the different drought statuses in the previous season. During spring season, the spatial distributions of drought severity with the largest occurrence probability given different drought statuses

Fig. 7 Spatial distribution of the predicted droughts with the largest occurrence probability in the Huai River basin during summer given the drought status in spring (**a** D4, **b** D3, **c** D2, **d** D1, **e** D0). Details of drought status can be referred to Table 1, and the *color bar* represents the value of SPEI

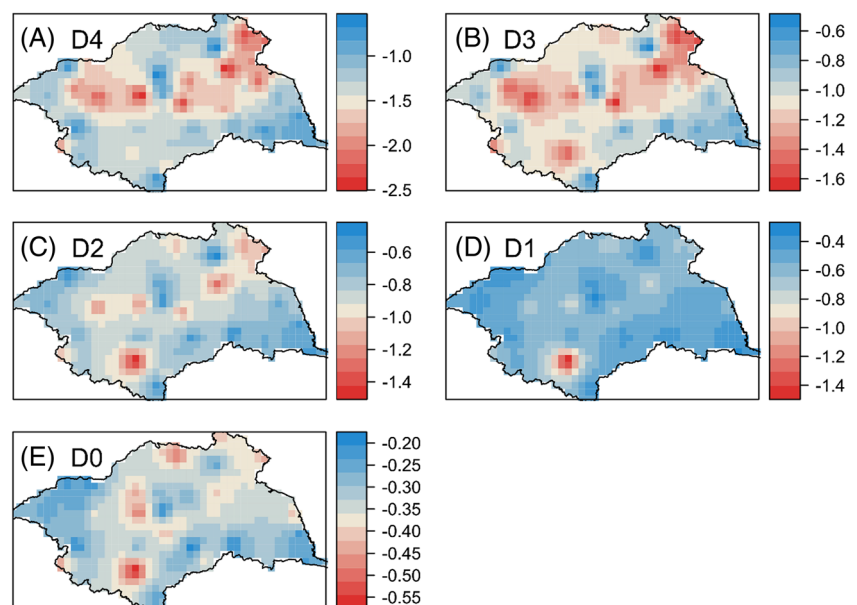
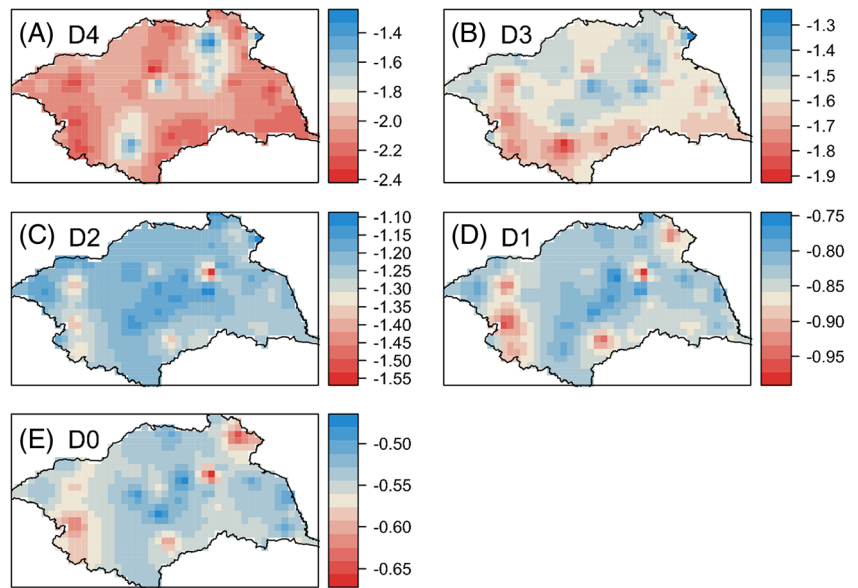


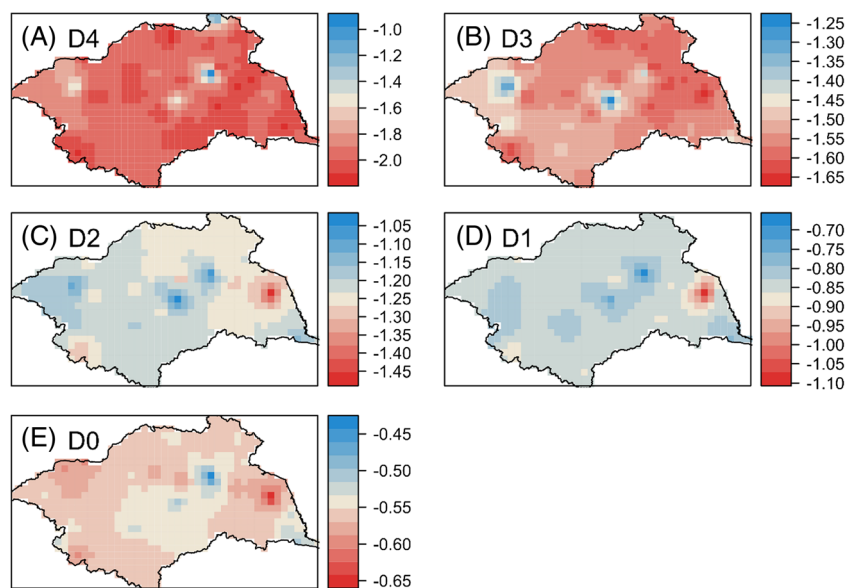
Fig. 8 Spatial distribution of the predicted droughts with the largest occurrence probability in the Huai River basin during autumn given the drought status in summer (a D4, b D3, c D2, d D1, e D0). Details of drought status can be referred to Table 1, and the color bar represents the value of SPEI



in winter were illustrated in Fig. 6. It can be seen from Fig. 6 that the larger area of the Huai River basin is dominated by persistently lasting droughts in spring when droughts in winter were less severe, and these results indicate that though the drought was not so severe in winter, considerable attention should be paid for mitigation of droughts in spring in that less severe droughts will still be persistent in larger areas in the Huai River basin. What is more, the severe drought in winter will be more likely to be persistent in the central part of the southern Huai River basin in spring, and as the wheat are always planted during winter and harvested during the late spring in the Huai River basin, then negative impacts can be expected from persistently lasting droughts on wheat production and it is particularly the case when there is a severe drought which occurred in winter in those regions.

Besides, extreme droughts in spring will be more likely to be durative in northern parts of the Huai River basin in summer (Fig. 7), except some regions in the central parts of the Huai River basin. As a major crop in the Huai River basin, the corns are always planted during summer. In this case, when there occurs extreme droughts in spring, effective planning of corn cultivation should be done to alleviate negative impacts of extreme droughts on corn production, and it is particularly true in that extreme droughts in summer will also be persistent with largest probability in autumn (Fig. 8) and winter (Fig. 9) in the northern parts of the Huai River basin. Furthermore, it can be seen from Figs. 7, 8, and 9 that droughts will be durative in a larger area in the Huai River basin in summer, autumn, and winter when the drought was more severe in the previous seasons, implying that the Huai River basin is vulnerable to the

Fig. 9 Spatial distribution of the predicted droughts with the largest occurrence probability in the Huai River basin during winter given the drought status in autumn (a D4, b D3, c D2, d D1, e D0). Details of drought status can be referred to Table 1, and the color bar represents the value of SPEI



long-lasting extreme drought in most parts of the drainage basin. It should be noted here that the forecasting of drought in the study is focused on the recovery stage; however, the statistical method introduced in the paper may have limited performance for the onset stage, and whether seasonal forecasting of global drought onset at local scale is essentially a stochastic forecasting problem has been questioned by Yuan and Wood (2013).

5 Conclusions

The Huai River basin is the major cropping area in China with a heavy responsibility of supply of agricultural products. However, frequent droughts inflict massive loss on agricultural production, showing apparent negative implications for social stability and food security. Good knowledge of drought behaviors means much for scientific management and planning of agricultural activities such as agricultural cultivation, agricultural irrigation, and also development of water-saving agriculture. In this case, the SPEI with the time scales of 3, 6, and 9 months has been analyzed to picture probability behaviors of droughts in the Huai River basin. With the copula functions to model the persistence property of drought, the conditional probability density functions were calculated and analyzed, and then the probabilistic seasonal drought forecasting models have been developed in the Huai River basin for each season based on the composite probability density distribution of the SPEI with the time scales of 3, 6, and 9 months. Using the seasonal data from 2011 to 2013, the probabilistic seasonal drought forecasting models have been validated, and results indicate that these models work well in the Huai River basin for each season. Generally, the variability of predicted seasonal drought is larger when more severe droughts occurred in the previous seasons. In this sense, occurrence of droughts with higher drought intensity can greatly enhance difficulty and unreliability of drought forecasting in the subsequent seasons.

Furthermore, spatial distributions of droughts with the largest occurrence probability in the Huai River basin for each season given the drought status in the previous season have been analyzed in this study. The results indicate that the Huai River basin is vulnerable to the extreme drought in most parts of the basin, such as the severe drought in winter will be highly probable to be durative in spring in the central part of the southern Huai River basin. The Huai River basin is densely populated and is also the principle cropping area in China; extreme droughts will have considerable impacts on the availability of water resources and also agricultural production. The results of the study provide theoretical references for the planning of crop cultivation and also for human mitigation to drought-induced losses in the Huai River basin, China.

Acknowledgments This work was financially supported by the National Science Foundation for Distinguished Young Scholars of China (Grant No.: 51425903), the Project supported by the Funds for International Cooperation and Exchange of the National Natural Science Foundation of China (Grant No.: 51210013), and the Natural Science Foundation of Anhui Province, China (Grant No.: 1508085MD65), and is fully supported by a grant from the Research Grants Council of the Hong Kong Special Administrative Region, China (Project No. CUHK441313). The last but not the least, our cordial gratitude should be extended to the editor, Prof. Dr. Jianping Li, and four anonymous reviewers for their professional comments and suggestions which are greatly helpful for their further improvement of the quality of this manuscript.

References

- AghaKouchak A (2014) A baseline probabilistic drought forecasting framework using standardized soil moisture index: application to the 2012 United States drought. *Hydrol Earth Syst Sci* 18(7):2485–2492
- Beguieria S, Vicente-Serrano SM (2013) SPEI: calculation of the standardised precipitation-*evapotranspiration* index. URL: <http://CRAN.R-project.org/package=SPEI>
- Bonaccorso B, Cancelliere A, Rossi G (2015) Probabilistic forecasting of drought class transitions in Sicily (Italy) using Standardized Precipitation Index and North Atlantic Oscillation Index. *J Hydrol* 526:136–150
- Cancelliere A, Mauro GD, Bonaccorso B, Rossi G (2007) Drought forecasting using the Standardized Precipitation Index. *Water Resour Manag* 21(5):801–819
- Chen YD, Zhang Q, Xiao MZ, Singh VP, Zhang S (2015) Probabilistic forecasting of seasonal droughts in the Pearl River basin. *China Stochastic Environmental Research and Risk Assessment* DOI: [10.1007/s00477-015-1174-6](https://doi.org/10.1007/s00477-015-1174-6)
- Droogers P, Allen R (2002) Estimating reference evapotranspiration under inaccurate data conditions. *Irrig Drain Syst* 16(1):33–45
- Duan K, Xiao W, Mei Y, Liu D (2014) Multi-scale analysis of meteorological drought risks based on a Bayesian interpolation approach in Huai River basin, China. *Stoch Env Res Risk A* 28(8):1985–1998
- FAO (2015) AQUASTAT website, Food and Agriculture Organization of the United Nations (FAO). Website accessed on [2015/05/28]
- Gao C, Zhang Z, Zhai J, Qing L, Mengting Y (2015) Research on meteorological thresholds of drought and flood disaster: a case study in the Huai River basin, China. *Stoch Env Res Risk A* 29(1):157–167
- Genest C, Rémillard B, Beaudoin D (2009) Goodness-of-fit tests for copulas: a review and a power study. *Insurance: Mathematics and Economics* 44(2):199–213
- Hargreaves GH (1994) Defining and using reference evapotranspiration. *J Irrig Drain Eng* 120(6):1132–1139
- Hofert M, Kojadinovic I, Maechler M, Yan J (2015) copula: multivariate dependence with copulas. R package version 0.999–13: URL: <http://CRAN.R-project.org/package=copula>.
- Kao SC, Govindaraju RS (2010) A copula-based joint deficit index for droughts. *J Hydrol* 380(1–2):21–134
- Ma F, Yuan X, Ye A (2015) Seasonal drought predictability and forecast skill over China. *Journal of Geophysical Research: Atmospheres* 120(16): 2015JD023185
- Madadgar S, Moradkhani H (2013) A Bayesian framework for probabilistic seasonal drought forecasting. *J Hydrometeorol* 14(6): 1685–1705
- Madadgar S, Moradkhani H (2014) Spatio-temporal drought forecasting within Bayesian networks. *J Hydrol* 512(0): 134–146
- Mishra AK, Singh VP (2010) A review of drought concepts. *J Hydrol* 391(1–2):202–216

- Nelsen RB (2006) An introduction to copulas. Springer Verlag, New York
- Niu J, Chen J, Sun L (2015) Exploration of drought evolution using numerical simulations over the Xijiang (West River) basin in South China. *J Hydrol* 526:68–77
- Salvadori G, De Michele C (2015) Multivariate real-time assessment of droughts via copula-based multi-site hazard trajectories and fans. *J Hydrol* 526:101–115
- Sanusi W, Jemain A, Zin W, Zahari M (2015) The drought characteristics using the first-order homogeneous Markov chain of monthly rainfall data in peninsular Malaysia. *Water Resour Manag* 29(5):1523–1539
- Shiau J (2006) Fitting drought duration and severity with two-dimensional copulas. *Water Resour Manag* 20(5):795–815
- Sklar A (1959) Fonctions de Répartition À N Dimensions Et Leurs Marges. *Publ Inst Stat Univ Paris* 8
- Van Loon AF, Laaha G (2015) Hydrological drought severity explained by climate and catchment characteristics. *J Hydrol* 526:3–14
- Vicente-Serrano SM, Beguería S, López-Moreno JI (2010) A multiscalar drought index sensitive to global warming: the Standardized Precipitation Evapotranspiration Index. *J Clim* 23(7):1696–1718
- Vicente-Serrano SM, Gouveia C, Camarero JJ, Beguería S, Trigo R, López-Moreno JI, Azorín-Molina C, Pasho E, Lorenzo-Lacruz J, Revuelto J, Morán-Tejeda E, Sanchez-Lorenzo A (2013) Response of vegetation to drought time-scales across global land biomes. *Proc Natl Acad Sci* 110(1):52–57
- Wang H, Kumar A (2015) Assessing the impact of ENSO on drought in the U.S. Southwest with NCEP climate model simulations. *J Hydrol* 526:30–41
- Wilhite DA (2000) Drought as a natural hazard: concepts and definitions.: in drought: a global assessment. Routledge Publishers, London, pp. 3–18
- Yan DH, Wu D, Huang R, Wang LN, Yang GY (2013) Drought evolution characteristics and precipitation intensity changes during alternating dry–wet changes in the Huang–Huai–Hai River basin. *Hydrol Earth Syst Sci* 17(7):2859–2871
- Yu M, Li Q, Hayes MJ, Svoboda MD, Heim RR (2014) Are droughts becoming more frequent or severe in China based on the standardized precipitation evapotranspiration index: 1951–2010? *Int J Climatol* 34(3):545–558
- Yuan X, Wood EF (2013) Multimodel seasonal forecasting of global drought onset. *Geophys Res Lett* 40(18):4900–4905
- Yuan X, Wood EF, Chaney NW, Sheffield J, Kam J, Liang M, Guan K (2013) Probabilistic seasonal forecasting of African drought by dynamical models. *J Hydrometeorol* 14(6):1706–1720
- Zhang Q, Qi T, Singh V, Chen Y, Xiao M (2015) Regional frequency analysis of droughts in China: a multivariate perspective. *Water Resour Manag* 29(6):1767–1787
- Zhang Q, Xiao M, Singh V, Chen X (2013a) Copula-based risk evaluation of droughts across the Pearl River basin. *China Theor Appl Climatol* 111(1–2):119–131
- Zhang Q, Xiao M, Singh V, Chen X (2013b) Copula-based risk evaluation of hydrological droughts in the East River basin, China. *Stoch Env Res Risk A* 27(6):1397–1406
- Zhang Q, Xiao M, Singh VP, Li J (2012) Regionalization and spatial changing properties of droughts across the Pearl River basin, China. *J Hydrol* 472–473(0): 355–366